Prepared for submission to JHEP

Krylov complexity in inverted harmonic oscillator

Seungjoo Baek

Department of Physics and Astronomy, Seoul National University, Seoul 08826, Korea

E-mail: seungjoobaek@snu.ac.kr

Abstract: Recently, the out-of-time-ordered correlator(OTOC) and Krylov complexity have been studied actively as a measure of operator growth. OTOC is known to exhibit exponential growth in chaotic systems, which was confirmed in many previous works. However, in some non-chaotic systems, it was observed that OTOC shows chaotic behavior and cannot distinguish saddle-dominated scrambling from chaotic systems. For K-complexity, in the universal operator growth hypothesis, it was stated that Lanczos coefficients show linear growth in chaotic systems, which is the fastest. But recently, it appeared that Lanczos coefficients and K-complexity show chaotic behavior in the LMG model and cannot distinguish saddle-dominated scrambling from chaos. In this paper, we compute Lanczos coefficients and K-complexity in an inverted harmonic oscillator. We find that they exhibit chaotic behavior, which agrees with the case of the LMG model. We also analyze bounds on the quantum Lyapunov coefficient and the growth rate of Lanczos coefficients and find that there is a difference with the chaotic system. Microcanonical K-complexity is also analyzed and compared with the OTOC case.

Contents

1 Introduction

Quantum chaotic systems play an important role in diverse areas of physics, ranging from condensed matter physics to quantum gravity. Especially, the relationship between complexity and holography has been unveiled in the last few years[1]. However, the definition of quantum chaos and the measure of quantum complexity are not fully established yet, and extensive research is going on in this field.

Several different measures of complexity were proposed. Among them, the most widely used one is level statistics of the Hamiltonian[2, 3]. Chaotic systems are known to exhibit Wigner-Dyson statistics, while integrable systems show Poisson statistics. But recently, more convenient measures based on operator growth emerged. The most extensively studied one is the out-of-time-ordered correlator(OTOC), which is defined as

$$C(t) = -\langle [V(0), O(t)]^2 \rangle_\beta \,. \tag{1.1}$$

By calculating commutators, it measures the overlap between the probe operator and the time-evolved reference operator. OTOC is calculated in many quantum systems[4–8], and is known to show exponential growth in early times in chaotic systems. The exponential growth rate is called the quantum Lyapunov coefficient. We will denote it as $\lambda_{L,T}$. T is the temperature. There exists a well-known bound on $\lambda_{L,T}$[9]:

$$\lambda_{L,T} \leq 2\pi T \,. \tag{1.2}$$

A relatively novel measure is Krylov complexity(K-complexity, in short). It measures how much the operator is spread in the operator Hilbert space during Heisenberg time

evolution. K-complexity has been calculated in many systems, including spin chain, SYK model and 2D CFTs[10–18]. Behavior in chaotic systems was studied; a universal operator growth hypothesis states that Lanczos coefficients grow linearly in chaotic systems, and that is the fastest growth[10]. The corresponding behavior for K-complexity is exponential growth. So, for chaotic systems,

$$\begin{aligned} b_n &\sim \alpha n\,, \\ K(t) &\sim e^{2\alpha t}\,. \end{aligned} \tag{1.3}$$

But this is valid only for small n and early times. b_n grows linearly until $n \sim S$ and shifts to the plateau phase. K-complexity turns to linear growth after $t \sim \log S$. S is the entropy of the system. For more details see section 2. Also, in [10], the new bound for $\lambda_{L,T}$ was proposed:

$$\lambda_{L,T} \leq 2\alpha_T^{(W)}\,. \tag{1.4}$$

Superscript (W) means that it was computed using the Wightman product. This was proved for infinite temperature and conjectured for finite temperature. It was also pointed out that

$$\alpha_T^{(W)} \leq \pi T\,, \tag{1.5}$$

So that

$$\lambda_{L,T} \leq 2\alpha_T^{(W)} \leq 2\pi T\,. \tag{1.6}$$

In the same paper, it was shown that for the large-q SYK model, the left side of (1.6) is saturated for all temperature ranges while the right side is saturated only in the zero temperature limit. We will return to (1.6) later and discover that the inverted harmonic oscillator situation is somewhat different.

Meanwhile, recently it was pointed out that saddle-dominated scrambling should be distinguished from chaos[4, 19]. Suppose an integrable system has a saddle point in phase space. In that case, exponential deviation of trajectories can occur near the saddle, but the entire system is not chaotic because it occurs only about the saddle point. Such integrable systems include Lipkin-Meshkov-Glick(LMG) model and inverted harmonic oscillator(IHO).[1] And in ref. [4], it was shown that OTOC grows exponentially in the LMG model. This is surprising because the exponential growth of OTOC was supposed to indicate chaos. In this context, OTOC is a 'poor' indicator of chaos. OTOC for IHO was calculated in [5, 19] and showed exponential growth in this model too.

So, it is natural to test whether K-complexity can distinguish saddle-dominated scrambling in non-chaotic systems from chaotic systems. In [22], this test was performed on the LMG model. The result showed that Lanczos coefficients and K-complexity behave

[1] Saddle-dominated scrambling can also appear in chaotic systems[20, 21], but we focus on integrable systems in this paper.

similarly to chaotic systems. Even microcanonical K-complexity away from the saddle energy seemed to detect the saddle. In this paper, we calculate K-complexity in an inverted harmonic oscillator system and show that K-complexity exhibits chaotic behavior.

Before turning to the next section, we make one remark. An inverted harmonic oscillator is not merely an interesting toy model for saddle-dominated scrambling; rather, it has physical significance in reality. For example, a relativistic particle near the black hole horizon pulled by force toward outside experiences inverted harmonic oscillator potential, which is related to chaotic behavior near the horizon[23]. The primary goal of our work is to investigate the nature of K-complexity, but our results may also have potential applications in realistic models.

This paper is organized as follows. In section 2, we review the Lanczos algorithm and the notion of K-complexity. In section 3, K-complexity for the inverted harmonic oscillator is numerically computed, and results are presented. Microcanonical K-complexity and oscillation of Lanczos coefficients are analyzed in the following section. In section 5, we conclude and discuss the implications of our result.

2 Review of Lanczos algorithm and K-complexity

In the Heisenberg picture, the operator goes through time evolution according to the Campbell-Baker-Hausdorff formula:

$$\mathcal{O}(t) = e^{iHt}\mathcal{O}_0 e^{-iHt} = \mathcal{O}_0 + it[H,\mathcal{O}_0] + \frac{(it)^2}{2!}[H,[H,\mathcal{O}_0]] + \cdots . \tag{2.1}$$

Consider the Hilbert space of operators and denote a vector in that space as $|A)$. We will use the following inner product, which is called the Wightman norm:

$$(A|B) = \langle e^{\beta H/2}A^\dagger e^{-\beta H/2}B\rangle_\beta \,, \tag{2.2}$$

where $\langle\cdots\rangle_\beta = Tr(e^{-\beta H}\cdots)/Tr(e^{-\beta H})$. β is an inverse temperature. Now, define Liouvillian superoperator as $\mathcal{L}|A) = |[H,A])$. Then nested commutators can be written as

$$|\bar{\mathcal{O}}_0) = |\mathcal{O}_0)\,, |\bar{\mathcal{O}}_1) = \mathcal{L}|\mathcal{O}_0)\,, |\bar{\mathcal{O}}_2) = \mathcal{L}^2|\mathcal{O}_0)\,, \cdots . \tag{2.3}$$

They span a subspace of operator Hilbert space called Krylov space. $\mathcal{O}(t)$ at arbitrary time t lies in this space. Dimension of Krylov space is denoted by $\mathcal{K}$, and it is bounded upwards: $1 \le \mathcal{K} \le D^2 - D + 1$ where D is a dimension of finite-dimensional Hilbert space. In this paper, we will deal with an infinite-dimensional system, so Krylov space will also be infinite-dimensional.

But the basis composed of $|\bar{\mathcal{O}}_i)$ is hard to handle because it is not orthonormal. We can apply Gram-Schmidt orthogonalization and obtain an orthonormal basis. The step-by-step procedure is as follows. Original reference operator is $|\mathcal{O})$.

1. Let $|\mathcal{A}_0) = |\mathcal{O})$. $|\mathcal{A}_i)$ will denote orthogonal vectors before normalization. Compute its norm $b_0 = \sqrt{(\mathcal{A}_0|\mathcal{A}_0)}$, and normalize : $|\mathcal{O}_0) = \frac{1}{b_0}|\mathcal{A}_0)$. $|\mathcal{O}_i)$ will denote orthonormal basis vectors.

2. Compute $|\mathcal{A}_1) = \mathcal{L}|\mathcal{O}_0)$. Calculate its norm and normalize it with $b_1 = \sqrt{(\mathcal{A}_1|\mathcal{A}_1)}\,, |\mathcal{O}_1) = \frac{1}{b_1}|\mathcal{A}_1)$.

3. For $n \geq 2$, $|\mathcal{A}_n) = \mathcal{L}|\mathcal{O}_{n-1}) - b_{n-1}|\mathcal{O}_{n-2})\,, b_n = \sqrt{(\mathcal{A}_n|\mathcal{A}_n)}\,, |\mathcal{O}_n) = \frac{1}{b_n}|\mathcal{A}_n)$.

4. Stop when $b_n = 0$.

Obtained orthonormal basis consisting of $|\mathcal{O}_i)$ is called Krylov basis. b_n are Lanczos coefficients. Now, we can expand the time-evolved operator at arbitrary time t using Krylov basis:

$$|\mathcal{O}(t)) = \sum_{n=0}^{\mathcal{K}-1} i^n \phi_n(t)|\mathcal{O}_n)\,. \tag{2.4}$$

Then $\phi_n(t)$ can be written as follows.

$$\phi_n(t) = i^{-n}(\mathcal{O}_n|O(t))\,. \tag{2.5}$$

Applying Heisenberg time evolution equation, we get a system of differential equations:

$$\partial_t \phi_n(t) = b_n \phi_{n-1}(t) - b_{n+1}\phi_{n+1}(t)\,, \tag{2.6}$$

with initial conditions $\phi_n(0) = \delta_{n0}\,, \phi_{-1}(t) = 0$.

Meanwhile, the Krylov basis can be viewed as a one-dimensional lattice. Initially, the reference operator is localized at $|\mathcal{O}_0)$, and spreads out to points with larger n during time evolution. $|\phi_n(t)|^2$ is a probability for the operator to be at position n at time t. Sum of the probability is always unity: $\sum_{n=0}^{\mathcal{K}-1} |\phi_n(t)|^2 = 1$. Then we can write the average position of the operator at time t as

$$K(t) = \sum_{n=0}^{\mathcal{K}-1} n|\phi_n(t)|^2\,. \tag{2.7}$$

This is the Krylov complexity(K-complexity in short).

In chaotic systems, it is known that Lanczos coefficients show asymptotically linear growth until it reaches a plateau phase:

$$b_n \sim \alpha n\,. \tag{2.8}$$

As n increases further, b_n experiences Lanczos descent and becomes zero at $n = \mathcal{K} - 1$. But the inverted harmonic oscillator system, which we will study below, won't exhibit this descent because it is infinite-dimensional. Correspondingly, for chaotic systems, K-complexity grows exponentially at early times:

$$K(t) \sim e^{2\alpha t}\,. \tag{2.9}$$

At time $t \sim \log S$, exponential growth turns to linear growth, and at $t \sim e^{\mathcal{O}(S)}$ K-complexity saturates. For chaotic systems saturation value would be $\mathcal{K}/2$ [15]. For integrable and free theories, K-complexity and Lanczos coefficients are supposed to grow slower than in chaotic systems.

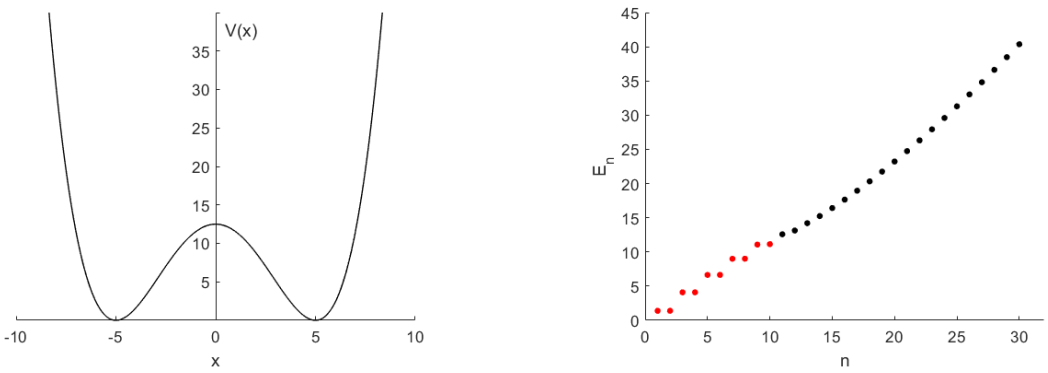

(a) (b)

Figure 1: (a) Potential $V(x)$ described in (3.1). (b) Spectrum of eigenvalues E_n until $n = 30$. A ground state corresponds to $n = 1$. Red ones, which are below $E_{saddle} = 12.5$, are almost but not exactly degenerate.

3 K-complexity in inverted harmonic oscillator

3.1 Inverted harmonic oscillator

In this paper, we focus on a one-dimensional inverted harmonic oscillator system, whose OTOC was studied in ref. [5, 19]. We will study the same system as [5]. The Hamiltonian is given by

$$\begin{aligned} H &= p^2 + V \\ V &= g\left(x^2 - \frac{\lambda^2}{8g}\right)^2 = -\frac{1}{4}\lambda^2 x^2 + gx^4 + \frac{\lambda^4}{64g}\,. \end{aligned} \tag{3.1}$$

We choose $\lambda = 2\,, g = 1/50$ for parameters. The shape of the potential and spectrum of energy eigenvalues are plotted in figure 1. There is a saddle at the center of the potential. We will denote nth energy eigenstate as $|n\rangle$. Since we will focus on a finite temperature system, eigenstates with sufficiently large n can be safely ignored when computing the Wightman product, because they are suppressed by the Boltzmann factor.[2] We will use $\hat{x}$ as an initial reference operator following [5].

3.2 K-complexity in infinite-dimensional system

In this subsection, we closely follow the method of [11], which we will exploit in this paper.

Calculating K-complexity for an infinite dimensional system is problematic because the Lanczos algorithm lasts forever. Here, we will stop the Lanczos algorithm at sufficiently big $n = N_{cut}$. This can be safely done because, at early times, the operator spread does not reach $|\mathcal{O}_n)$ with big n. More quantitatively, we will always make sure that the difference between $\sum_{n=0}^{N_{cut}-1} |\phi_n(t)|^2$ and 1 does not exceed 10^{-4}.

[2] We kept eigenstates until $n = 119$.

To perform Lanczos algorithm, we need to calculate Wightman inner product $(\mathcal{A}_n|\mathcal{A}_n)$:

$$\begin{aligned}(\mathcal{A}_n|\mathcal{A}_n) &= \frac{Tr(e^{-\beta H/2}\mathcal{A}_n^\dagger e^{-\beta H/2}\mathcal{A}_n)}{Tr(e^{-\beta H})} \\ &= \frac{\sum_{m,l} e^{-\beta(E_m+E_l)/2}\langle m|\mathcal{A}_n^\dagger|l\rangle\langle l|\mathcal{A}_n|m\rangle}{Z}\,,\end{aligned} \tag{3.2}$$

where $Z = \sum_m e^{-\beta E_m}$. In the second step we used completeness relation $\sum |l\rangle\langle l| = 1$. Now consider the structure of $|\mathcal{A}_n)$. $|\mathcal{A}_n)$ is defined as a linear combination of nested commutators and an initial reference operator. Every term will contain one $\hat{x}$ and some power of H multiplied left and right sides of $\hat{x}$. A total number of H multiplied in a term cannot exceed n because the highest order term in $|\mathcal{A}_n)$ will come from n times nested commutator. Then we can write matrix elements as follows:

$$\begin{aligned}(\mathcal{A}_n)_{ml} &= \sum_{k=0}^{n}\sum_{a+b=k} D_{ab}^n E_m^a E_l^b \langle m|\hat{x}|l\rangle\,, \\ (\mathcal{O}_n)_{ml} &= \sum_{k=0}^{n}\sum_{a+b=k} C_{ab}^n E_m^a E_l^b \langle m|\hat{x}|l\rangle\,.\end{aligned} \tag{3.3}$$

Evidently, $C_{ab}^n = D_{ab}^n/b_n$. Since our eigenfunctions are all real and $\hat{x}$ is a Hermitian, it can be easily seen that

$$(\mathcal{A}_n^\dagger)_{ml} = (\mathcal{A}_n)_{lm}\,. \tag{3.4}$$

This leads to following simplification:

$$(\mathcal{A}_n|\mathcal{A}_n) = \frac{\sum_{m,l} e^{-\beta(E_m+E_l)/2}(\mathcal{A}_n)_{ml}^2}{Z}\,. \tag{3.5}$$

To compute C_{ab}^n and D_{ab}^n, substitute (3.3) to the definition of $|\mathcal{A}_n)$(see step 3 of Lanczos algorithm). It gives recurrence relations:

$$\begin{aligned}D_{ab}^n &= C_{a-1,b}^{n-1} - C_{a,b-1}^{n-1} \qquad (a+b=n\,,n-1) \\ D_{ab}^n &= C_{a-1,b}^{n-1} - C_{a,b-1}^{n-1} - b_{n-1}C_{a,b}^{n-2} \qquad (a+b\le n-2)\,.\end{aligned} \tag{3.6}$$

In this way, we can compute the Wightman product and implement the Lanczos algorithm. The summary of our numerical calculation procedure is as follows.

1. Obtain eigenvalues E_n and eigenvectors $|n\rangle$ numerically.
2. Calculate $\langle m|\hat{x}|l\rangle$ for various values of m and l.
3. Implement Lanczos algorithm using the recurrence relation (3.6) and results of step 2. Compute K-complexity with resulting Lanczos coefficients.

Numerical results are presented in the following subsection.

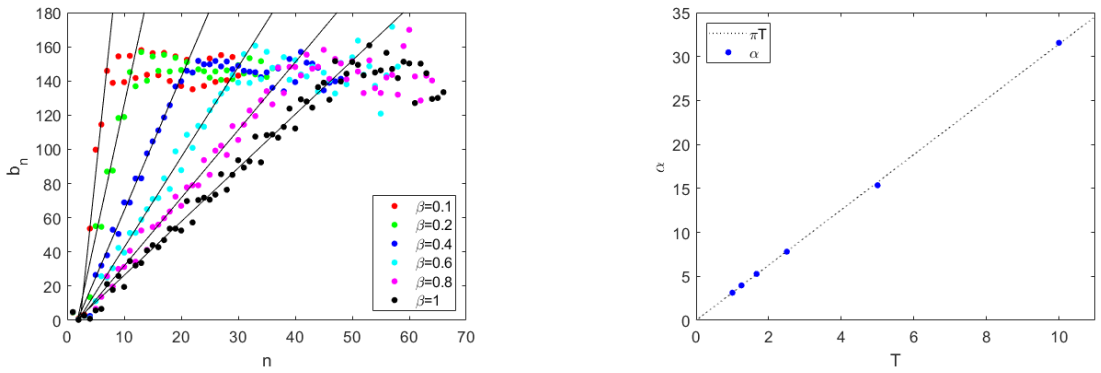

(a) (b)

Figure 2: (a) Lanczos coefficients for $\beta = 0.1 \sim 1$. Only datas before the divergence of b_n are used. Linear fits are also shown. (b) Linear growth rate of b_n, $\alpha_T^{(W)}$, is plotted against temperature T. Line πT is also shown. It can be seen that (1.5) is saturated in this temperature range up to numerical precision.

3.3 Numerical results

Numerical results are presented in figure 2. Before analyzing the results, we will make one remark. The original Lanczos algorithm is known to suffer from numerical instability. Since we only needed to calculate Lanczos coefficients with relatively small n, it was enough for us to use data before b_n started to diverge. But in models with high entropy, for example, the SYK model, we need to use more precise algorithms like Full Orthogonalization(FO) or Partial Re-Orthogonalization(PRO). For details see [12].

Figure 2a shows Lanczos coefficients for temperature range $\beta = 0.1 \sim 1$. In all cases, it can be seen that b_n linearly increases for small n and shifts to the plateau phase. The value n where b_n shifts increase with β, but the value of b_n at the plateau remains unchanged with temperature. To our knowledge, this constantness of plateau has not been investigated in detail. We leave this to future work. In figure 2b, we plotted α as a function of T. It appears that in our temperature range, the bound (1.5) is saturated up to numerical precision.

Figure 3 shows log-plot of corresponding K-complexity growth. For high-temperature cases, exponential growth is not clearly visible. It is because, as we can see in figure 2a, there are too few Lanczos coefficients in the linear growth phase for high-temperature cases. Indeed, we can see that, as temperature goes down, more Lanczos coefficients are contained in a linear growth phase, and exponential growth becomes more pronounced.

To sum up, we conclude that Lanczos coefficients and K-complexity behave in an inverted harmonic oscillator as if it was a chaotic system. Some comments are in order. First, our result differs from OTOC, where OTOC does not exhibit chaotic behavior at low temperature[5]. This behavior originates from the microcanonical nature of K-complexity and OTOC. We will study this in detail in section 4. Secondly, using the result of [5], we can test the inequality (1.6) for $\beta = 0.1\,, 0.2$. We summarized relevant values in table 1. As we can see, the right side of (1.6) is saturated, while the left side is trivially satisfied(up

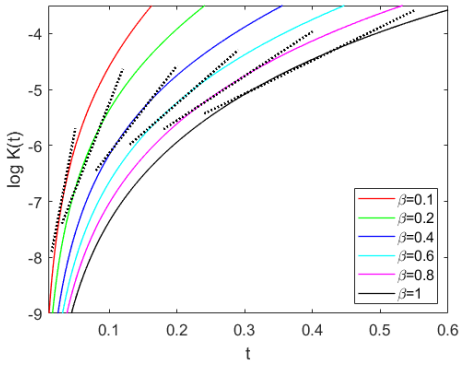

Figure 3: Log plot of K-complexity for $\beta = 0.1 \sim 1$. Black dotted lines mark exponential growth period of $K(t)$. Their slope is set to $2\alpha_T^{(W)}$, where $\alpha_T^{(W)}$ was found in figure 2.

β	$\lambda_{L,T}$	$2\alpha_T^{(W)}$	$2\pi T$
0.1	~ 2	63.1	62.8
0.2	~ 2	30.7	31.4

Table 1: Quantum Lyapunov coefficients $\lambda_{L,T}$, exponential growth rate of K-complexity $2\alpha_T^{(W)}$, and $2\pi T$ for $\beta = 0.1\,, 0.2$. $\lambda_{L,T}$ is extracted from [5].

β	0.1	0.2	0.4	0.6	0.8	1
S	3.04	2.45	1.74	1.34	1.11	0.963
$\log S$	1.11	0.897	0.553	0.296	0.105	-0.0377

Table 2: Shannon entropy for $\beta = 0.1 \sim 1$.

to numerical precision. $2\alpha_T^{(W)}$ appears to be slightly bigger than $2\pi T$ for $\beta = 0.1$, but it is in the range of numerical error. We are currently focusing on the rough tendency.). This is in stark contrast with the large-q SYK model, where the left side is saturated for all temperature ranges, and the right side is trivially satisfied[10]. We leave the resolution of this difference to future work. It may be related to the difference between chaotic systems and saddle-dominated non-chaotic systems. Finally, we can compute the Shannon entropy of the system numerically and compare it with our results. Shannon entropy is given by

$$S = -\sum_n (e^{-\beta E_n}/Z) \log(e^{-\beta E_n}/Z)\,, \tag{3.7}$$

and numerical values are given in table 2. As we can see, $S \sim 1$ and $\log S \sim 0.1$. We can confirm that, in figure 2, b_n shows linear growth until n reaches roughly $S \sim 1$. The exponential growth of K-complexity ceases around the time $\log S \sim 0.1$.

4 Microcanonical K-complexity

4.1 Microcanonical K-complexity in inverted harmonic oscillator

Microcanonical K-complexity, introduced in [13], probes operator growth in the specific energy sector of the operator. It enables us to analyze the contributions of different energy states to the original K-complexity. We first review the arguments of [13], then present numerical results for the inverted harmonic oscillator.

The reference operator can be expanded as follows:

$$|\mathcal{O}) = \sum_{i,j} \langle E_i|\mathcal{O}|E_j\rangle |E_i\rangle\langle E_j| \,. \tag{4.1}$$

Applying Liouvillian, we get

$$\mathcal{L}|\mathcal{O}) = \sum_{i,j} (E_i - E_j)\langle E_i|\mathcal{O}|E_j\rangle |E_i\rangle\langle E_j| \,. \tag{4.2}$$

As we can see in (4.1) and (4.2), Liouvillian does not mix different average energy sectors. If we define average energy observable as $\mathcal{E}|\mathcal{O}) = \frac{1}{2}|\{H, \mathcal{O}\})$, $[\mathcal{E}, \mathcal{L}] = 0$ and average energy is conserved. This means that we can implement the entire Lanczos algorithm in a fixed average energy sector and study operator growth. All we have to do is to change the inner product as follows:

$$(A|B)_E = \frac{1}{Z} \sum_{E_n = E} \langle n|e^{H\beta/2} A^\dagger e^{-H\beta/2} B|n\rangle \,. \tag{4.3}$$

The rest of the analysis is identical with section 3.

Figure 4 shows microcanonical Lanczos coefficients at $\beta = 0.4$ for $E_{1,2} = 1.4$, $E_{11} = 12.6$ and $E_{20} = 23.2$. It can be seen that they show similar behavior with original Lanczos coefficients at $\beta = 0.4$ in all cases. The growth rate and plateau value are approximately the same. Considering that saddle point energy is $E_{saddle} = 12.5$, we conclude that Lanczos coefficients show chaotic behavior not only near the saddle but also away from the saddle. This agrees with [22]. Microcanonical K-complexities can be computed directly, and results are presented in figure 5. One can easily confirm that they show chaotic behavior. Also, microcanonical K-complexity gets bigger as the mode gets higher. Thus, modes near the saddle don't necessarily dominate the entire K-complexity, considering the high-temperature limit where Boltzmann factors are suppressed. This is different from the LMG model[22], where microcanonical K-complexity near the saddle dominates the entire K-complexity. Also, microcanonical K-complexity explains the difference with OTOC, which was pointed out in section 3.3. According to [5], microcanonical OTOCs show strong exponential growth only in the range $n = 9 \sim 13$(around saddle point energy), while lower modes and higher modes do not show initial exponential growth. So thermal OTOC exhibits exponential growth only at high temperatures. But in our case, since microcanonical Lanczos coefficients and K-complexities exhibit chaotic behavior even away from the saddle, original Lanczos coefficients and K-complexities show chaotic behavior in a broad temperature range.

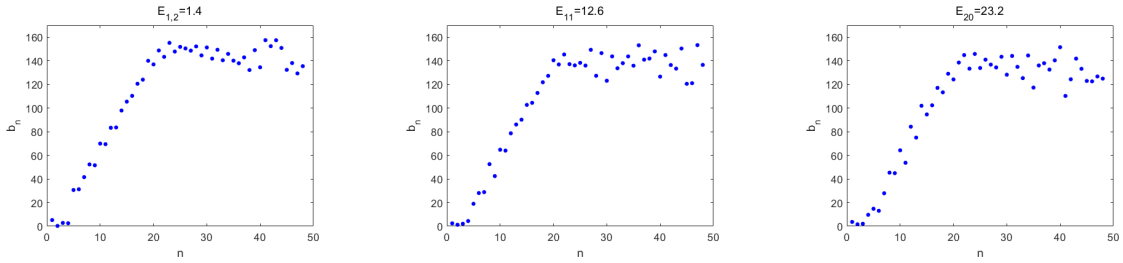

(a) $E_{1,2} = 1.4$ (b) $E_{11} = 12.6$ (c) $E_{20} = 23.2$

Figure 4: Microcanonical Lanczos coefficients at $\beta = 0.4$ for $E_{1,2} = 1.4$, $E_{11} = 12.6$ and $E_{20} = 23.2$. Only data before the divergence of b_n are used. Oscillation of b_n is more pronounced in E_{20} mode than in E_{11} mode.

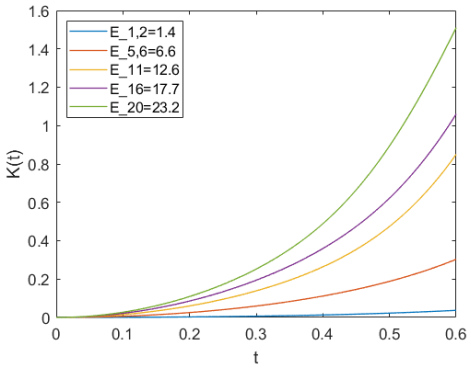

Figure 5: Microcanonical K-complexity at $\beta = 0.4$ for $E_{1,2} = 1.4$, $E_{5,6} = 6.6$, $E_{11} = 12.6$, $E_{16} = 17.7$, and $E_{20} = 23.2$ mode. Microcanonical K-complexity gets bigger as the mode gets higher.

4.2 Oscillation of Lanczos coefficients

Looking carefully at figure 2 and figure 4, we can see that in some cases b_n experiences oscillation, as if b_n of even and odd n behave separately. This phenomenon was also observed in previous works, and has been argued to be related to the behavior of autocorrelation function $C(t)$[11, 22, 24, 25]. Autocorrelation function is defined as $C(t) = \phi_0(t)$. We will briefly review the argument presented in [22] and apply it to our case.

Suppose Lanczos coefficients can be written in a form

$$b_n = f(n) + (-1)^n g(n)\,. \tag{4.4}$$

Plugging it in into Schrodinger equation leads to the solution

$$\phi_0(t) \sim g(n(u = t/2)) + O(g^2)\,, \tag{4.5}$$

where

$$u = \int \frac{dn}{2f(n)}\,. \tag{4.6}$$

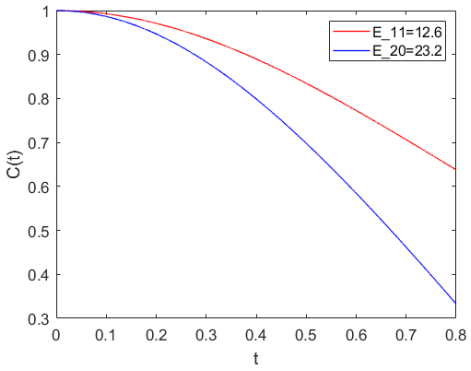

Figure 6: Microcanonical autocorrelation function $C(t)$ at $\beta = 0.4$ for E_{11} mode(red line) and E_{20} mode(blue line). $C(t)$ for E_{20} mode decreases faster than E_{11} mode.

From this, it follows that if the oscillation of b_n is big, it corresponds to bigger g, and $C(t)$ will change rapidly. If the oscillation of b_n is small, $C(t)$ will change slowly.

Figure 6 shows microcanonical $C(t)$ for E_{11}, E_{20} mode at $\beta = 0.4$. Corresponding Lanczos coefficients are in figure 4b and figure 4c. As we can see in figure 4, oscillation is more pronounced in E_{20} case(until $n \sim 25$, after that other instabilities dominate). According to the preceding discussion, $C(t)$ for E_{20} should change rapidly than E_{11} case. Indeed, we can confirm this in figure 6. In early times, $C(t)$ for E_{20} decreases faster than that of E_{11}. Here we focused on only early-time behavior because, at late times, other instabilities of b_n will become important.

5 Conclusion and Discussion

In this paper, we computed Lanczos coefficients b_n and K-complexity $K(t)$ of an inverted harmonic oscillator system, which is non-chaotic but shows saddle-dominated scrambling. As a result, we found that b_n shows linear growth for small n, and $K(t)$ has an exponential growth period in early times. Since this behavior is supposed to appear in chaotic systems, we conclude that K-complexity cannot distinguish chaos and non-chaotic saddle-dominated scrambling. This is in agreement with [22]. We also found that in our case, the right side of (1.6) is saturated, while in the chaotic system left side is saturated[10]. We anticipate that this phenomenon could be related to the difference between chaos and saddle-dominated scrambling.

Microcanonical K-complexity was analyzed in section 4. We saw that microcanonical b_n and $K(t)$ show chaotic behavior not only near the saddle but also away from the saddle, which is in agreement with [22]. This is in contrast with microcanonical OTOC case[5], where microcanonical OTOC exhibits exponential growth only near the saddle energy. The oscillation of Lanczos coefficients was analyzed using the result of [22].

As mentioned in the introduction, quantum chaos and complexity are becoming increasingly important in physics; studying more precise diagnostic of complexity, which can distinguish chaos and saddle-dominated scrambling, will be fruitful. To do that, we need to

classify more non-chaotic systems with the saddle-dominated scrambling. We leave these problems to future work.

Acknowledgments

We appreciate Prof. Sangmin Lee for valuable discussions during the progress of this work.

References

[1] Leonard Susskind. Three Lectures on Complexity and Black Holes. SpringerBriefs in Physics. Springer, 10 2018.

[2] L. F. Santos and M. Rigol, *Onset of quantum chaos in one-dimensional bosonic and fermionic systems and its relation to thermalization*, *Phys. Rev. E* **81** (Mar, 2010) 036206, [arXiv:0910.2985].

[3] E. Rabinovici, A. Sánchez-Garrido, R. Shir and J. Sonner, *Krylov complexity from integrability to chaos*, *JHEP* **07** (2022) 151 [2207.07701].

[4] T. Xu, T. Scaffidi, and X. Cao, *Does scrambling equal chaos?*, *Phys. Rev. Lett.* **124** (2020), no. 14 140602, [arXiv:1912.11063].

[5] K. Hashimoto, K.-B. Huh, K.-Y. Kim, and R. Watanabe, *Exponential growth of out-of-time-order correlator without chaos: inverted harmonic oscillator*, *JHEP* **11** (2020) 068, [arXiv:2007.04746].

[6] T. Akutagawa, K. Hashimoto, T. Sasaki, and R. Watanabe, *Out-of-time-order correlator in coupled harmonic oscillators*, *JHEP* **08** (2020) 013, [arXiv:2004.04381].

[7] K. Hashimoto, K. Murata, and R. Yoshii, *Out-of-time-order correlators in quantum mechanics*, *JHEP* **10** (2017) 138, [arXiv:1703.09435].

[8] S. Pasterski and H. Verlinde, *Chaos in celestial CFT*, *JHEP* **08** (2022) 106, arXiv:2201.01630 [hep-th].

[9] J. Maldacena, S. H. Shenker, and D. Stanford, *A bound on chaos*, *JHEP* **1608**, 106 (2016) [arXiv:1503.01409 [hep-th]].

[10] Daniel E. Parker, Xiangyu Cao, Alexander Avdoshkin, Thomas Scaffidi, and Ehud Altman, *A universal operator growth hypothesis*, *Phys. Rev. X* **9**, 041017 (2019).

[11] Shiyong Guo, *Operator growth in SU(2) Yang-Mills theory*, arxiv:2208.13362.

[12] E. Rabinovici, A. Sánchez-Garrido, R. Shir, and J. Sonner, *Operator complexity: a journey to the edge of Krylov space*, *JHEP* **06** (2021) 062, [arXiv:2009.01862].

[13] A. Kar, L. Lamprou, M. Rozali, and J. Sully, *Random matrix theory for complexity growth and black hole interiors*, *JHEP* **06** (2022) 016, [arXiv:2106.02046].

[14] P. Caputa and S. Datta, *Operator growth in 2d CFT*, *JHEP* **12** (2021) 188, [arXiv:2110.10519].

[15] E. Rabinovici, A. Sánchez-Garrido, R. Shir, and J. Sonner, *Krylov localization and suppression of complexity*, *JHEP* **03** (2022) 211, [arXiv:2112.12128].

[16] V. Balasubramanian, P. Caputa, J. Magan, and Q. Wu, *Quantum chaos and the complexity of spread of states*, *Phys. Rev. D* **106**, no. 4, 046007 (2017), arXiv:2202.06957.

[17] A. Dymarsky and M. Smolkin, *Krylov complexity in conformal fi eld theory*, *Phys. Rev. D* **104** (2021), no. 8 L081702, [arXiv:2104.09514].

[18] S.-K. Jian, B. Swingle, and Z.-Y. Xian, *Complexity growth of operators in the SYK model and in JT gravity*, *JHEP* **03** (2021) 014, [arXiv:2008.12274].

[19] A. Bhattacharyya, W. Chemissany, S. S. Haque, J. Murugan, and B. Yan, *The Multi-faceted Inverted Harmonic Oscillator: Chaos and Complexity*, *SciPost Phys. Core* **4** (2021) 002, [arXiv:2007.01232].

[20] M. Feingold and A. Peres, *Regular and chaotic motion of coupled rotators*, *Physica D: Nonlinear Phenomena* **9** (1983), no. 3 433-438.

[21] R. H. Dicke, *Coherence in spontaneous radiation processes*, *Phys. Rev.* **93** (Jan, 1954) 99-110.

[22] B. Bhattacharjee, X. Cao, P. Nandy, and T. Pathak, *Krylov complexity in saddle-dominated scrambling*, *JHEP* **05** (2022) 174, [arXiv:2203.03534].

[23] K. Hashimoto and N. Tanahashi, *Universality in Chaos of Particle Motion near Black Hole Horizon*, *Phys. Rev. D* **95**, no. 2, 024007 (2017) [arXiv:1610.06070 [hep-th]].

[24] D. J. Yates, A. G. Abanov, and A. Mitra, *Lifetime of Almost Strong Edge-Mode Operators in One-Dimensional, Interacting, Symmetry Protected Topological Phases*, *Phys. Rev. Lett.* **124** (2020), no. 20 206803, [arXiv:2002.00098].

[25] D. J. Yates, A. G. Abanov, and A. Mitra, *Dynamics of almost strong edge modes in spin chains away from integrability*, *Phys. Rev. B* **102** (2020), no. 19 195419, [arXiv:2009.00057].